

Survey of Electric Propulsion Capability

Kenn E. Clark*

Princeton University, Princeton, N. J.

Introduction

AFTER nearly two decades of research and development, and several recent and ongoing successful tests in space, electric propulsion systems are emerging which are capable of fulfilling the secondary propulsion requirements of initial station acquisition, stationkeeping, attitude control, and modest repositioning, as well as providing primary propulsion for a wide range of interesting missions. Further, system reliability has now advanced sufficiently to project electric propulsion to the threshold of several flights, where it will be an integral part of functioning spacecraft.

Many excellent reviews of the historical development and status of electric propulsion have appeared in the literature.¹⁻⁷ The purpose of this paper is to provide the spacecraft designer with sufficient information regarding the recent progress and present capability of the several types of electric propulsion systems to enable him to optimize his selection for a particular mission. To this end, each of four major classes of electric thruster (electrothermal, plasma, colloid, and ion) is briefly described and the distinct programs in each class reviewed. The emphasis is on performance capability, development status, program goals, and technology improvement. Adequate references are provided for a more detailed examination of each thruster program.

Electrothermal Thrusters

Electrothermal thrusters use resistance elements to convert electricity to heat, thereby increasing the enthalpy of the propellant to a level comparable to and sometimes greater than that of a chemical rocket. The principal advantage of this type of thruster is its simplicity, not only in the thrust chamber, which may consist of only one or more concentric tubes, but also in the associated mass feed system, which is an outgrowth of the highly developed cold gas feed systems, and the power processor, which in some cases is not even required. The uncoupling of the working fluid from the energy input allows a wide choice of propellants, depending on specific requirements regarding molecular weight, storability, and

ease of handling. An additional advantage of certain types of electrothermal thrusters is that they can be pulsed, which makes them suitable for attitude control and possibly east-west stationkeeping.

The primary drawback of this class of thruster is that the propellant temperature is limited to the maximum wall temperature, which at present translates into an effective exhaust velocity less than 10^4 m/sec (specific impulse less than 10^3 sec).[†] In addition, the efficiency is also limited by the energy which must be deposited in nonthermal modes in the propellant such as molecular rotation, vibration, and dissociation. This "frozen flow" loss alone can dictate a maximum efficiency of anywhere from 10% to near 100%, depending on the propellant and the pressure and temperature within the thruster.⁹

Within these constraints, several viable electrothermal thruster systems have been developed which are capable of a variety of modest, low-total-impulse missions. Initial activity in electrothermal thruster development focused on steady-state, fairly long thermal transient (several minutes) configurations where propellants such as H_2 , N_2 , NH_3 and the biowaste products— CO_2 , H_2O , CH_4 —were fed to the chamber through multiple heating passages. The first electric thruster in space was of this type,¹⁰ and an 8000-hr-lifetime at effective exhaust velocities of 6560 and 3140 m/sec (670 and 320 sec) has been demonstrated using H_2 and NH_3 devices, respectively.¹¹ However, little research effort on the steady-state electrothermal thruster remains because of the storability problem of hydrogen, the lack of interest in biowastes due to the diminished manned space-flight program, and the general availability of higher performance systems. Nevertheless, the nitrogen resistojet still offers modest fail-safe improvement over a cold gas system, and ammonia provides further system performance gains, due to its storability.

In the pulsed class of electrothermal thrusters, two subclasses have been developed. In the first of these, power is continuously supplied to a chamber and nozzle configuration of large thermal inertia. Thrust pulses are obtained then by

Kenn E. Clark is a Research Engineer in the Electric Propulsion Laboratory of the Aerospace and Mechanical Sciences Department of Princeton University. He received his B. S. E. and M. S. E. degrees in Aeronautical Engineering from the University of Michigan in 1961 and 1962 respectively, and his Ph. D. degree in Aerospace and Mechanical Sciences from Princeton University in 1969. His present work involves the study of acceleration processes in magnetoplasmadynamic discharges and the application of these electromagnetic devices to space propulsion, high-power plasmadynamics lasers, arc physics and energy conversion. He is a member of the AIAA, serves on the Electric Propulsion Technical Committee, and is an Associate Editor of the *Journal of Spacecraft and Rockets*.

Presented as Paper 74-1082 at the AIAA/SAE 10th Propulsion Conference, San Diego, California, October 21-23, 1974; submitted November 25, 1974; revision received July 9, 1975. The author acknowledges with appreciation the many contributions and helpful discussions rendered by J. Burkhart, L. Dailey, B. Free, W. Guman, J. Molitor, C. Murch, J. Perel, K. Pugmire, R. Worlock, and S. Zafran. In addition, the paper benefited from preliminary examinations and comments by K. Atkins, H. Kaufman, W. Kerslake, F. Mead, W. Owens, W. von Jaskowsky, and P. Wilbur. This work was supported by NASA NGL 31-001-005.

Index category: Electric and Advanced Space Propulsion.

*Research Engineer. Member AIAA.

[†]Specific impulse here will be defined in the conventional way, i.e., thrust divided by weight flow of propellant, but Greenwood has shown⁸ that specific impulse is more properly defined in terms of propellant mass flow and, as such, is equal numerically to and has the units of the effective exhaust velocity. Throughout this paper, effective exhaust velocity will be used, with the specific impulse given after it in parentheses.

simply pulsing the propellant, although duty cycles are limited to less than 2%, due to the finite thermal capacity of the thruster.³ This configuration was flight tested, but it is not now under active study.

In the second subclass of pulsed thrusters, both power and propellant are pulsed in a configuration of very low thermal inertia. This device provides a fast heatup time as well as the capability for continuous operation, with firing times as long as 20 days recorded.¹² Used primarily with ammonia, several of these thruster systems have been flown, successfully providing orbit control of small spacecraft. Due to their proven reliability, this type of electrothermal thruster is still under active study and refinement.

Considerable interest has recently been shown in the electrothermal hydrazine thruster as an alternative to the conventional hydrazine thruster. The conventional hydrazine thruster, using a catalyst bed for the decomposition of the liquid hydrazine, has been utilized extensively in the past on operational spacecraft. The thrust level of typically 1-50 N is particularly suited for initial orbit acquisition and small stationkeeping functions. Although the conventional hydrazine thruster has been used for three-axis attitude control on some spacecraft, the minimum impulse bit from this thruster is typically one to two orders of magnitude greater than the optimum for attitude control of small spacecraft.¹³ In addition, this thruster is troubled by deterioration of the catalyst bed, with a resulting degradation of specific impulse, impulse bit reproducibility, and lifetime.

Electrothermal hydrazine thrusters avoid the catalyst problem by electrically heating the hydrazine to a temperature high enough (550 K) to trigger the exothermic decomposition reaction. The principal advantage of this approach is the ability to reach the low thrust levels and impulse bits unattainable with the catalytic devices, and the resulting possibility of combining high-thrust catalytic hydrazine thrusters with low-thrust electrothermal hydrazine thrusters on the same mission while using the same mass feed system. The electrothermal hydrazine thruster is under active development in both the United States and Europe.

Pulsed Ammonia Thruster (AVCO)

The pulsed ammonia thruster or ammonia resistojet is an extremely simple device. In one configuration, used on the ATS series spacecraft, the heater and heat exchanger is a single straight rhenium tube with the nozzle at one end. In another configuration, the interior heater element is a coiled filament. Recent modifications of this latter type consist of an encapsulated filament with a spiral heat exchanger foil. A typical complete thruster is shown in Fig. 1. For a complete multithruster system, ammonia vapor is fed to the thrusters from a "preplenum" tank located inside the propellant tank. By drawing the heat of vaporization from the stored propellant and from the spacecraft waste heat, only ammonia vapor is delivered to the thrusters. A downstream plenum is used to minimize pressure fluctuations. On several recent configurations, mass feed systems such as described above have been capable of delivering ammonia vapor to the thruster at more than one pressure. This allows a thrust variation (in discrete steps) of over an order of magnitude by ground command switching of the delivery pressure. No power conditioning is necessary as these simple thrusters operate directly from spacecraft voltage.

Performance

For a two-thrust-level system, typical thrusts of 44.5 and 133 μN (10 and 30 μlb) are delivered at an input power of 5 w. The effective exhaust velocity for this system is approximately 1320 m/sec (135 sec) as compared to an effective exhaust velocity for cold ammonia of 690 m/sec (70 sec).

In the recent larger four-thrust-level systems, thrusts of 133, 445, 1330 and 4450 μN (30, 100, 300 and 1000 μlb) are available at an input power of 6.5 w. Effective exhaust

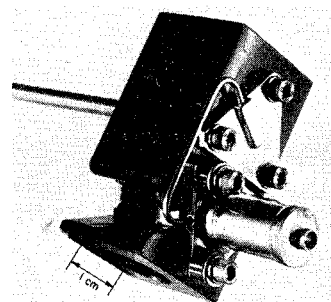


Fig. 1 Ammonia resistojet (AVCO).

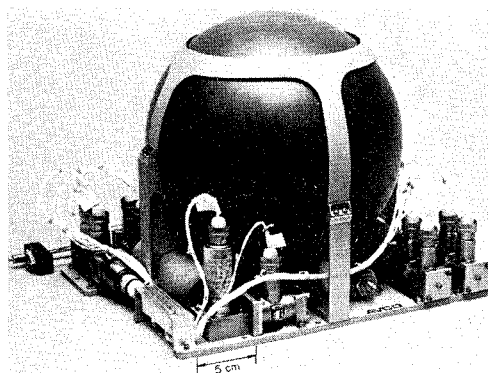


Fig. 2 Ammonia resistojet system (AVCO).

velocities for this device are about 1470 m/sec (150 sec) at the 133 μN thrust, 1760 m/sec (180 sec) for thrust levels of 445 and 1330 μN , and 1620 m/sec (165 sec) for a thrust of 4450 μN .

System status

Ammonia thrusters have been used on more than a dozen flights since 1965. The two-thrust-level system discussed here has been used successfully on four Naval Research Laboratory (NRL) spacecraft launched in 1971. Thrust from these devices, of which each spacecraft had two, was measured in orbit to be within 15% of ground measured thrust.

The four-thrust-level system will be used on several NRL spacecraft with an anticipated launch date of 1975.¹² The complete thrust system is shown in Fig. 2. Each spacecraft will have four thrusters and about 4.5-5.5 kg of ammonia, which will give a total impulse capability of approximately 6600-9900 N-sec (1480-2220 lb-sec).

Hydrazine Thruster (TRW)

The electrothermal hydrazine thruster developed by TRW consists of a 0.51-cm-diam by 1.27-cm-long thrust chamber followed by a standard nozzle of 15° half-angle divergence and an area ratio of 50.¹⁴ The interior of the chamber is packed with approximately 60, 0.5-cm-diam platinum screens to aid the decomposition process. The chamber is connected to the propellant feed valve by a small injector tube surrounded by a supporting perforated cylinder, which acts as a thermal barrier to minimize conduction losses from the chamber. A Nichrome heater element is wrapped around the thrust chamber to provide the decomposition temperature initially. The power required is minimal. For duty cycles below 5%, a power of only 3-5 w is necessary; for duty cycles from 5% to steady state, the element can be turned off after the initial start, with sufficient heat provided by the exothermic reaction itself. The thruster can be operated using spacecraft voltage directly without any power conditioning. The complete insulated thruster and valve assembly is shown in Fig. 3.

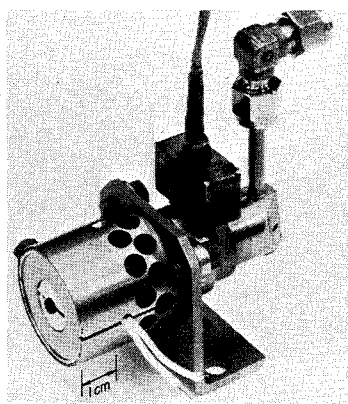


Fig. 3 Electrothermal hydrazine thruster (TRW).

Table 1 Performance of electrothermal hydrazine thruster

Thrust, mN (mlb)	22.2-310 (5-70)
Effective exhaust velocity, m/sec(sec)	
—pulsed	1620-2110 (165-215)
—steady	2250 (230)
Power, w	5
Minimum impulse bit for 50 msec pulse, N-sec (lb-sec)	$< 2.2 \times 10^{-3}$ ($< 0.5 \times 10^{-3}$)

Performance

Performance of the electrothermal hydrazine thruster in both the pulsed and steady-state modes of operation is summarized in Table 1.

The thrust level is roughly one to two orders of magnitude less than that of the catalytic thruster. Thus, since the supply pressure of the hydrazine is approximately the same as is used for catalytic thrusters, the possibility exists of a dual-thruster system with a common mass feed system where the higher-thrust catalytic device is used for orbit acquisition while the lower-thrust electrothermal unit provides the small reproducible impulse bits necessary for attitude control.

The particular value of specific impulse obtained in the pulse mode depends on both the pulse width and the duty cycle. It is lowest for short pulses and low-duty cycles where heat loss to the thruster absorbs a larger percentage of the heat of decomposition. The heat loss can, of course, be reduced by maintaining the thruster at a higher holding temperature between pulses, but this requires additional power. The power level quoted in Table 1 maintains the thruster at approximately 810 K as compared to a measured steady-state temperature of 1190-1220 K. The steady-state velocity is reached only after run times of 1-2 min.

System status

A cycle life test has been conducted using developmental hardware. The test was voluntarily terminated after more than 10^6 cycles with pulse widths of 10-150 msec. Subsequent inspection of the thruster showed no evidence of injector plugging.

At present, an 89 mN thruster is in the test evaluation stage. Upon demonstration of a 10^6 cycle life with this unit, the total impulse capability will be greater than 4000 N-sec (900 lb-sec), which is adequate for long-term attitude control of geosynchronous satellites. Future plans are to conduct a parallel life test on both electrothermal and catalytic thrusters.

Hydrazine Thruster (AVCO)

The AVCO electrothermal hydrazine thruster is similar in size and performance to the TRW unit. Up to two years ago,

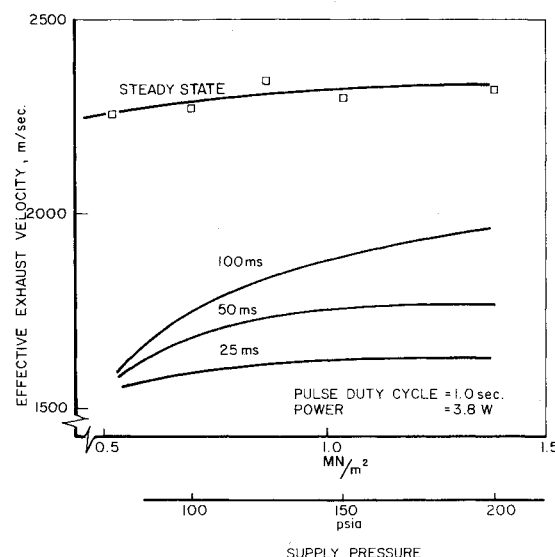


Fig. 4 Electrothermal hydrazine thruster performance (AVCO).

thrusters in the 130-450 mN (30-100 mlb) thrust class were developed. These devices required 3-5 w to initiate the decomposition and were also self-sustaining once started. As with the TRW unit, 10^6 cycles from a holding temperature have been demonstrated. In addition, 10^5 starts from ambient temperature have been achieved.¹² A summary of available exhaust velocity as a function of hydrazine supply pressure for both pulsed and steady-state operation is shown in Fig. 4. The thrust range for these data is 133-266 mN (30-60 mlb).

Technology

Developmental efforts in the electrothermal hydrazine program are proceeding in two directions. One goal is to establish operation with lower freezing point propellants than hydrazine (275 K).¹⁵ This would decrease the thermal control requirements on the spacecraft while providing commonality with bipropellant feed systems.

The second task is to upgrade the thrust to the 2-20 N (approximately 0.5-5 lb) level. Performance at the 4.4 N (1.0 lb) thrust level has now been demonstrated in both pulsed and steady-state modes.¹² This thruster requires approximately 10 w starting power and operates with an effective exhaust velocity comparable to the smaller engines.

Pulsed Plasma Thrusters

Plasma propulsion involves the use of an electrical discharge to drive a large current through the working fluid. The interaction of this current with a properly configured magnetic field (either externally applied or self-generated) produces volumetric body forces which directly accelerate the propellant. The advantage of this approach over electrothermal thrust production lies in the ability to produce kinetic energy directly, without first depositing the power in the thermal mode. By comparison, electrothermal thrusters are fundamentally limited to chamber temperatures, and therefore exhaust velocities, which are compatible with structural materials.

Although some plasma thrusters have been considered for primary propulsion, the general lack of a large, lightweight power supply to drive multikiloamp currents has necessarily limited the present interest in this concept to pulsed devices. Here, one or more capacitors are steadily charged from the spacecraft power source and periodically discharged through the thruster in a pulse of high current. The impulse bit thus generated can be made large or small, depending on the size of the capacitor supply.

The ability to produce small, precise, reproducible impulse bits at effective exhaust velocities of several thousand meters

per second makes pulsed plasma thrusters ideally suited for long-term attitude control and east-west stationkeeping of both three-axis-stabilized and spin-stabilized satellites. Increasing the total energy per pulse and the pulse repetition rate produces a time-average thrust large enough to satisfy north-south stationkeeping requirements. It should be noted that varying the pulse repetition rate provides a throttling capability without altering either the effective exhaust velocity or the thrust efficiency.

Pulsed plasma thrust generation has been demonstrated with gaseous, liquid, and solid propellants. Of these, the most attractive at present (and the only type to be developed to flight status) is the solid-propellant thruster. In this device, a high current discharge is generated across the face of a solid, in most cases Teflon. Energy transfer from the discharge depolymerizes the Teflon, with the vaporized species subsequently accelerated through a nozzle by electromagnetic body forces. The advantages of the solid propellant are its extreme simplicity and ease of operation on a spacecraft; valves, feed lines, and external tankage are not required.

Thrusters of the solid-propellant ablative type have been flown successfully on the LES-6 satellite. Launched in 1968, this spin-stabilized satellite used four pulsed ablative thrusters for east-west stationkeeping. One of these thrusters has logged more than 8900 hr of stationkeeping operation at synchronous altitude.

The present program in pulsed plasma thrusters is almost completely centered on the ablative type, with thrusters under development in both the micro-Newton and milli-Newton thrust range.

Pulsed Ablative Microthruster

The Teflon pulsed ablative microthruster is shown schematically in Fig. 5. The main energy storage capacitor is joined to the anode and cathode by special low-inductance, low-resistance connections. The rod of Teflon propellant is pressed against a fuel retaining shoulder in the anode by a constant force spring. Since both the exposed Teflon surface and the surface behind this shoulder are ablated with each discharge, the spring maintains a fresh propellant surface at the discharge chamber independent of thruster attitude, thermal environment, absence of gravity, or duration of thruster operation.

Generation of an impulse bit involves charging two separate capacitors: the energy storage capacitor already described, usually charged to over 1000 v, and the smaller, discharge initiating capacitor, usually charged to several hundred volts. This latter capacitor is connected to an igniter plug in the thruster nozzle. Because of the vacuum in the interelectrode gap prior to the discharge, both voltages are maintained until a firing command signal triggers the discharge initiation circuit. This causes a small discharge at the igniter plug, which in turn provides sufficient electrical conductivity for the main gap to break down, allowing the energy storage capacitor to deliver energy into the plasma.

Power conditioning for this type of thruster consists of a transformer, which converts the 28 v d.c. spacecraft voltage into a 5 kHz current source for charging the capacitors. To limit the time at which the energy storage capacitor is at high voltage and thereby to extend its life, the capacitors are charged only immediately prior to the time at which the impulse bit is desired.

The LES-6 microthruster had a main energy storage capacitor of $2 \mu\text{F}$ which was charged to 1360 v and a discharge initiating capacitor of $1 \mu\text{F}$, which was charged to 550 v.¹⁶ Each thruster was fired once every 6 sec with capacitor charging occurring only over the last 1.2 sec of the offtime. A particularly interesting feature of this thruster was a dual-nozzle side-by-side arrangement whereby half of the propellant was expended in one electrode pair and half in the other (Fig. 6). Each of the two electrode assemblies in each nozzle had its own discharge initiating capacitor, giving each

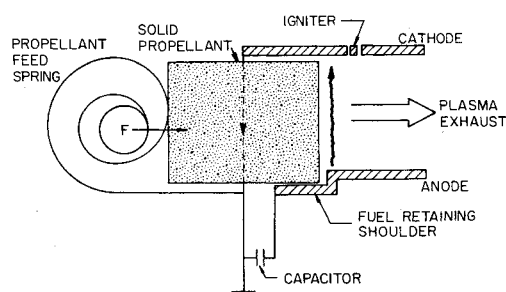


Fig. 5 Schematic of pulsed ablative microthruster.

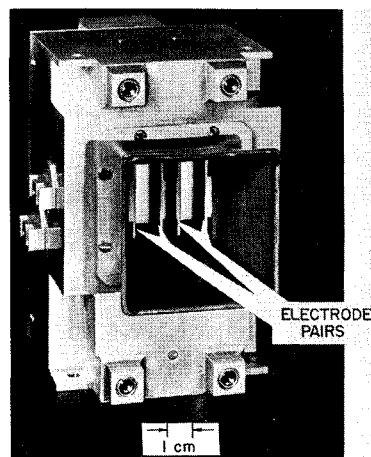


Fig. 6 LES-6 pulsed ablative microthruster (Fairchild).

thruster dual redundancy. A flip-flop circuit in the power conditioner alternately switched between electrode pairs of each thruster.

Three programs are now in progress to develop flight systems using pulsed ablative microthrusters of considerably different operational capabilities.

SMS Microthruster (Fairchild)

An ablative microthruster system has been developed for use on the spin-stabilized Synchronous Meteorological Satellite (SMS).¹⁷ Two of these thrusters can be used to provide east-west stationkeeping and spin axis precession control. The thrusters will be subjected to a sustained acceleration of 13 g's in the direction of the thrust axis for the full five-year mission operation.

The basic structure of the SMS thruster is similar to the LES-6 thruster except that it is considerably scaled up in performance—111 $\mu\text{N}\cdot\text{sec}$ (25 $\mu\text{lb}\cdot\text{sec}$) impulse bit, 1780 N·sec (400 lb·sec) total impulse as compared to 26.7 $\mu\text{N}\cdot\text{sec}$ (6 $\mu\text{lb}\cdot\text{sec}$) impulse bit, 285 N·sec (64 lb·sec) total impulse for the LES-6 thrusters. Unlike the LES-6 thruster, each nozzle has only one electrode pair, but this pair has two solid state igniter plugs in the cathode which are alternately triggered on successive discharges. Each of the two main energy storage capacitors has been increased to 4 μF with a slightly greater charging voltage of 1450 v. To maximize capacitor life, a sensor detects the time at peak voltage and delays initiation of the charging cycle for a time dependent on the satellite spin rate (50-110 rpm). In this way, the time at peak voltage never exceeds 40 msec, and the total time under high-voltage stress drops from approximately 2920 h to 178 h.

LES-9 Microthruster (MIT Lincoln Lab)

The Lincoln Experimental Satellite LES-9 is a 454-kg advanced communication spacecraft due to be launched in November 1975 with a five-year mission goal. Six ablative microthrusters will be incorporated (three on the east face and three on the west face), each capable of operation at repetition

rates of either 1 pps or 6 pps.¹⁸ At the lower pulse rate, the six thrusters will be used for east-west stationkeeping and three-axis attitude control; at the higher pulse rate, additional spacecraft power will be used to operate three thrusters on a face simultaneously for orbit acquisition and station changes.

Each thruster has two Teflon fuel bars, which are mounted and fed parallel to the thruster axis but whose faces are cut such that the normal to the cut face is directed outward 30° from the thruster axis. An electrode pair and nozzle arrangement is mounted on each of these two canted fuel rod faces so that each thruster can produce impulse bits directed at either +30° or -30° with respect to the thruster axis. A single 17- μ F oil-filled capacitor charged to 1540 v is capable of providing either thrust chamber of a given thruster with a 12- μ sec current pulse peaking at 18 ka. The discharge is initiated in the thrust chambers by one of two redundant spark plugs, alternately driven by 2- μ F capacitors charged to 625 v. Power conditioning efficiency from a spacecraft voltage of 15-30 v is 80% at a power level of 60 w.

TIP-2 Microthruster (Johns Hopkins)

The Navy Transit Improvement Program (TIP-2) satellite will make use of two ablative microthrusters for drag compensation. Impulse bits of 400 μ N-sec (90 μ lb-sec) will be provided with a total impulse capability of 2450 N-sec (550 lb-sec).^{7,19}

Performance

Table 2 compares the performance parameters of the various microthrusters with those of the early LES-6 thruster. Unless otherwise specified, the values are given on a per thruster basis.

It should be noted that the SMS thruster shows an equivalent steady-state thrust throttling capability of more than 2 to 1 without changing either effective exhaust velocity or efficiency. Similarly, the LES-9 thruster produces a factor of six thrust increase without affecting other performance variables.

The overall system efficiency of these microthrusters is low due to the low effective exhaust velocity, which results in turn from the small energy expended per pulse. As the energy expended per discharge increases, the overall efficiency is seen to increase. This trend continues in the large-thrust ablative systems discussed in the next section.

System status

The SMS system, shown in Fig. 7, is a fully flight-qualified system, having passed shock, vibration, high g, and thermal vacuum tests. The complete system shown, including integrated power conditioning and logic, has a mass of 4.1 kg, of which 0.45 kg is propellant. A lifetest of 1.31 (10^7)

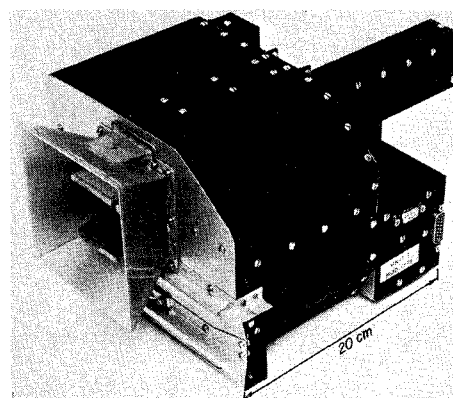


Fig 7 SMS microthruster system (Fairchild).

discharges has been conducted without incident. A detailed reliability analysis of the complete thruster system gives a five-year worst case reliability of 0.92. Without the main discharge capacitor, this figure increases to 0.98.

The LES-9 microthruster system is also flight-qualified, having passed vibration and shock tests and having demonstrated a life in excess of 3.4(10^7) pulses. In addition, the energy storage capacitor and the spark plugs have been life tested more than once without problems. Based on these tests, the extrapolated life of the energy storage capacitor is greater than 10^{11} discharges. A complete thruster has a mass of 6.59 kg, of which 0.75 kg is fuel, 1.93 kg is the capacitor, 0.91 kg is power conditioning and discharge initiation circuitry, and 3 kg is structure.

Milli-Newton Thruster (Fairchild)

The pulsed ablation microthruster has been scaled up to higher thrust levels in this program, whose immediate goal is to produce a 4.4-mN thrust device (1 mlb) with an effective exhaust velocity of 14,700 m/sec (1500 sec) and an overall efficiency of 30%.²⁰ This translates into a desired power-to-thrust ratio of 24.5 w/mN.

Initial data from this program have displayed an interesting range of performance values. Using discharge energies of 171-750 joules, the following performance data have been recorded on a direct measuring thrust balance: thrusts of 1.5-7.1 mN (0.35-1.63 mlb), effective exhaust velocities of 9350-50,600 m/sec (950-5160 sec), power-to-thrust ratios of 24.7-58.4 w/mN, impulse bits of 2.9-32.4 mN-sec (0.65-7.3 mlb-sec), and efficiencies of 18-53%.^{20,21}

A significant portion of the effort to develop an ablative thruster at this performance level has been expended on capacitor development and Teflon feed techniques. Recently, capacitors rated at 7.45 joules/kg have been shown capable of

Table 2 Ablative microthruster performance (flight systems)

	LES-6	SMS	LES-9	TIP-2
Discharge energy, joules	1.85	8.4	20	20
Impulse bit, μ N-sec	26.7	111	307	400
(μ lb-sec)	(6.0)	(25)	(69)	(90)
Mass expelled per shot, μ g	≈ 14	≈ 23	≈ 28	≈ 75
Effective exhaust velocity, m/sec	1960	4900	10,800	5400
(sec)	(200)	(500)	(1100)	(500)
Equivalent steady thrust, μ N	17.8	89-200	307/1840	400 max
(μ lb)	(4.0)	(20-45)	(69/414)	(90)
Bus power, w	2.5	8.7-14.6	25/150	30 max
Power-to-thrust, w/mN	140	97.7	80.8	75
Repetition rate, sec ⁻¹	0.16	0.83-1.83	1 / 6	single pulse/1
Total number of pulses	1.2(10^7)	1.6(10^7)	3.4(10^7)	6(10^6)
Total impulse, N-sec	285	1780	11,800	2450
(lb-sec)	(64)	(400)	(2650)	(550)
Approximate system efficiency, %	0.7	3.1	6.6	3.7

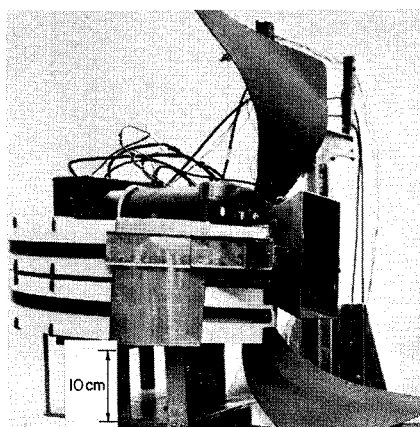


Fig. 8 Milli-Newton thruster (Fairchild).

Table 3 Milli-Newton ablative thruster performance

Thrust, mN (mlb)	3.98 (0.894)
Effective exhaust velocity, m/sec (sec)	17,600 (1790)
Power input, w	137
Power-to-thrust ratio, w/mN	34.4
Thrust efficiency, %	31.5
Overall system efficiency, %	25.3
Total impulse capability, N-sec (lb-sec) ^a	167,000 (37,500)

^a Not life tested to date.

absorbing a steady power input of 130 w while radiating to a 27.2°C sink.²²

Also, a method of storing and feeding the Teflon rods in helical loops has recently been demonstrated, which should allow compact storage of the propellant required for high total impulse applications—typically 167,000 N-sec (37,500 lb-sec).

The completed milli-Newton thruster system is shown in Fig. 8. It is capable of delivering 170,000 N-sec (38,200 lb-sec) and has a mass of 22.7 kg, of which half is propellant. Table 3 summarizes the performance of this thruster system to date.¹⁹

Technology

To decrease the system mass and improve the reliability of the pulsed ablative thruster over the entire range of thrust levels, high-energy-density capacitors (>22 joules/kg) are needed. Capacitors capable of providing 10⁶ discharges with an energy density as high as 88 joules/kg now exist but suffer oil leakage when exposed to a vacuum. Methods of hermetically sealing these capacitors are at present under study.¹⁹

Improved thruster performance may be realized from a program to investigate the effects of seeding the Teflon propellant or using alternate thermoplastics. To date, seeding has produced little positive effect, but a 60% increase in effective exhaust velocity and a 20% increase in efficiency have been recorded with other thermoplastic propellants.²¹

Throughout all of the pulsed plasma thruster performance data reported here, the trend toward improved performance for higher energy discharges is apparent. An isolated test of the LES-9 thruster provides an interesting example. Increasing the energy per pulse from 20 joules to 80 joules at a fixed power input of 25 w (a decrease in the pulse rate by a factor of four is implied), the equivalent steady thrust increases by 22%, the effective exhaust velocity by 32%, and the total impulse by 36%.

Further improvements may be realized from other investigations where the pulse energy is increased to the multikilojoule level for pulse times of the order of 1 msec. In these longer discharges, the acceleration process achieves, after some 10's of μ sec, a steady phase similar to steady-state

magnetoplasmadynamic (MPD) arc accelerators.^{23,24} Although still in the research stage, the "quasi-steady" accelerator may prove to have an overall efficiency greater than its short pulse and steady-state counterparts since 1) the lossy transients associated with the initiation and decay of the current are reduced to small fractions of the total pulse, and 2) the quasi-steady accelerator can operate in the multimewatt power regime inaccessible to strictly steady-state devices. For example, tests with argon propellant have shown that the fraction of the total input power that is lost to the anode of a quasi-steady MPD accelerator decreases from 45% at a power level of 0.4Mw to less than 10% as the quasi-steady power is increased to 15Mw.²⁵

Other techniques for plasma acceleration recently have been brought to promising levels of performance. The low power MPD accelerator is a steady-state external magnetic field device which accelerates a xenon plasma in a 400-v, 1.2-amp discharge.²⁶ At this 480-w power level, a thrust of 16.6 mN (3.7 mlb), an effective exhaust velocity of 21,600 m/sec (2200 sec), and an efficiency of 37% have been recorded.²⁷

As an alternative to the low power, steady plasma accelerator, the pulsed inductive thruster electromagnetically accelerates slugs of gaseous propellant which are injected over a flatcoil face. Early performance measurements showed an effective exhaust velocity of 14,700 m/sec (1500 sec) at an efficiency of 18%.²⁸ This program is now directed toward the use of two opposing coils in a configuration resulting in a greater conversion of magnetic field energy into plasma streaming energy.²⁹

Colloid Thrusters

A colloid engine produces thrust by accelerating electrically charged particles through an electrostatic field. The propellant, which is usually glycerol doped with sufficient sodium iodide or lithium iodide to provide the necessary conductivity, is fed through a small hollow needle biased positively at several thousand volts, (Fig. 9). The combination of feed pressure, surface tension, and electrostatic forces at the tip of the needle forms small ($\approx 100\text{\AA}$ diameter) positively charged multimolecular droplets, which are subsequently accelerated in the electrostatic field between the needle and a negatively biased extractor electrode surrounding the needle tip. A separate shield electrode, placed between the needle tip and the extractor, is maintained at the positive potential of the needle to protect the latter from secondary electron bombardment due to positively charged particles impacting the extractor. Many of these needle-shield-extractor combinations, each of which produces approximately 10 μ N (2.2 μ lb) thrust, are usually operated in parallel to achieve a desired total thrust level. An electron source is used to neutralize the positive droplets downstream of the extractor.

The principal advantage of a colloid thruster over an ion engine is its larger thrust for a given input power, which is

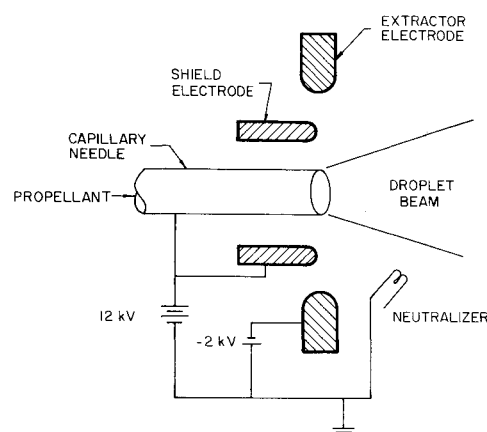


Fig. 9 Schematic of colloid emitter.

Table 4 Colloid ADP performance specifications

Thrust, mN (mlb)	4.45 (1.0)
Thrust variation, %	± 2
Effective exhaust velocity, m/sec (sec)	14,700 (1500)
System weight, kg	< 22.7
System power, w	< 70
Total impulse, N-sec (lb-sec)	≈ 164,650 (37,000)
Lifetime, yr	7
On-off cycles	5000
Average beam divergence, half-angle deg	< 15

directly related to the mass-to-charge ratio of the expended particles. In an ion engine the mass-to-charge ratio is 200 (atomic mass units per unit charge, amu/e) for the single mercury ion, while the mass-to-charge ratio for a colloid is typically 10^4 amu/e, the ionization energy expenditure of both being roughly the same. For a given power, this higher thrust translates into a less stringent demand on the total thrusting time. Another advantage of the colloid thruster is the ability to achieve throttling by trading thrust for specific impulse.

On the other hand, colloid thrusters are limited by this same mass-to-charge ratio and by the impressed voltages to effective exhaust velocities of about 20,000 m/sec (2000 sec). In addition, since there is in actuality a distribution in the mass-to-charge ratio of the accelerated particles, there is a similar spread in the exhaust velocity with its associated inefficiency.

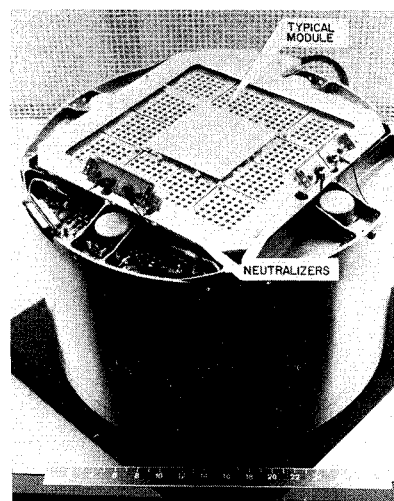
Within these limitations, the colloid thruster seems well suited for certain geocentric missions, especially stationkeeping of geosynchronous satellites, where the lower power-to-thrust ratio at desirable specific impulses can be best utilized in these power-limited environments.

Colloid thruster technology during the sixties led to the development of a flight-qualified, three-needle array microthruster system—35.6 μ N (8 μ lb) thrust, 9300 m/sec effective exhaust velocity (950 sec)⁷—which was subsequently not flown due to cancellation of the satellite program. In 1970, the Colloid Advanced Development Program (ADP) was initiated by the Air Force to demonstrate the feasibility of colloid propulsion for future mission applications. The performance goals of this radiation-hardened, 4.45 mN (1 mlb) thrust system are shown in Table 4.

Colloid ADP Thruster (TRW)

The colloid ADP thruster, which has been discussed extensively in the literature,^{30,31} consists of an array of 432 needles, each producing approximately 10 μ N (2.2 μ lb) thrust. For ease of handling and construction, the 0.36-mm-o.d., 0.13-mm-i.d. needles are arranged in 12 modules of 36 needles each. A separate 1.6-mm-o.d. shield electrode surrounds each needle, while the extractor electrode is a plate for each module with 36 holes of 3.2-mm-diam located so as to be concentric with each of the 36 needles. The needle and shield electrode are both nominally maintained at +12 kv, while the extractor is at -2 kv. Neutralization of the positively charged exhaust beam is accomplished by thermal electron emission from a 0.05-mm-diam, 6.3-cm-long tungsten wire mounted to the side and immediately downstream of the plane of the extractor electrode. A second neutralizer assembly is included for redundancy. The thruster unit, showing the 12 modules and two neutralizers, is shown in Fig. 10.

Centrally located between the 12 thruster modules is the mass-flow distribution manifold and flow controller assembly. The propellant (glycerol with 19.4% by weight of sodium iodide) is stored within the base of the thruster unit (Fig. 10) in a positive expulsion bellows. Flow to the needles is initiated and regulated by heating a zeolite canister desorbing CO₂, which controls a ball valve in the main propellant line. Cooling the zeolite closes the ball valve, stopping the

**Fig. 10 Colloid ADP thruster (TRW).****Table 5 Colloid ADP thruster performance**

	Design	Typical	Best
Thrust, mN (mlb)	4.4 (1.0)	4.4 (1.0)	4.6 (1.05)
Effective exhaust velocity, m/sec (sec)	14,700 (1500)	13,385 (1365)	15,100 (1540)
Thruster efficiency, %	70	58	72
Needle voltage, kv	12.3	12.2	12.7
Needle current, mamp	3.8	4.15	3.7
Beam power, w	46.7	50.6	47.0
Mass flow rate, μ g/sec	303	332	310
Power-to-thrust ratio, w/mN	10.6	11.5	10.2
Average mass-to-charge ratio, amu/e	7650	9290	8050

propellant flow, and in addition places the remaining propellant downstream of the valve in tension, which results in a retraction or "pull back" of the propellant from the needle tips, thereby reducing the propellant surface area exposed to vacuum.

The power conditioner is relatively simple, consisting of an input filter, an inductive energy storage converter to supply the high voltages, and a 20 kHz inverter to provide thruster temperature control, canister heat, and neutralizer heat. Only seven external commands are necessary to operate the complete system, with eight telemetry channels also provided by the unit. The power conditioner has been packaged and has an efficiency of 84.4% at room temperature and 28 v d.c. input.

Performance

Thruster performance data are compared to the design conditions in Table 5. It is seen that under isolated conditions, the design goal has been reached, but performance more typically lies below this for reasons to be discussed.

Endurance tests have been performed on various components of the thruster system. One of the most important of these was a 4350-hr-test on one of the 12, 36-needle modules.³² Inspection of the module at the end of the test revealed no evidence of approaching failure, although both thrust and effective exhaust velocity had decreased by roughly 15%, due to material buildup on the needles and needle erosion, causing an increase in the mass-to-charge ratio of 20%. Recently, a second life test of a module has begun. As of the time of this writing, over 5500 hr of operation had been logged. Other tests have included a 1000-hr test of a bread-board model of the complete, 12-module thruster and accelerated life tests on neutralizers which showed a projected neutralizer life of 24,000 hr.

Table 6 Colloid ADP thruster system mass and power summary

	Mass	Power	
Thruster	1.5 kg	46.7 w	(Beam)
		2.0	(Heater)
Neutralizer	---	5.0	
Feed system	3.0	2.0	
Power conditioning and control	4.5	12.6	
Structure	2.5	---	
Propellant	11.3	---	
Total	22.8 kg	68.3 w	

System status

The ADP thruster is at present in the prototype configuration. The total projected system mass of 22.8 kg is expected to be distributed as shown in Table 6. This includes 11.3 kg of propellant which, at an expulsion efficiency of 95% and an effective exhaust velocity of 14,700 m/sec (1500 sec), translates into a total impulse of 158,000 N-sec (35,500 lb-sec). The projected distribution of power commensurate with reaching the overall system design goals is also presented in Table 6.

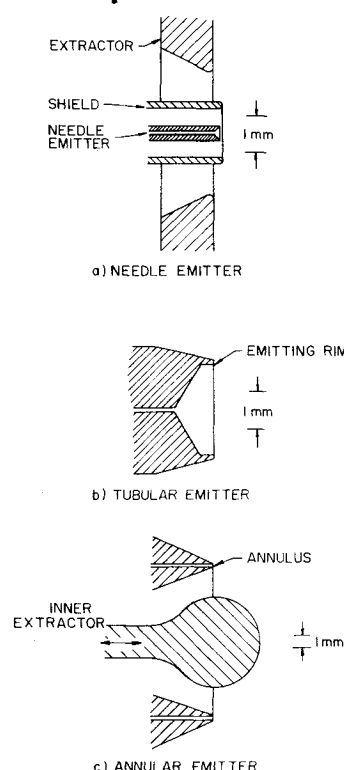
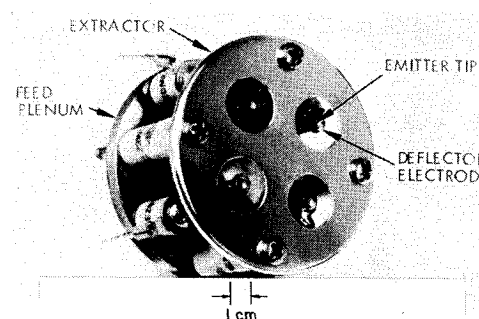
Five-year program goals for colloid propulsion are aimed at a demonstration of a 10,000-hr lifetime at the specified performance conditions with flight-qualified hardware. A space flight test is anticipated in 1977 or 1978.

Technology

Performance measurements and life tests have indicated certain problem areas yet remaining with the ADP thruster, as well as the apparent resolution of former difficulties. The principal problems arise at the needle tips, where contamination from either the propellant, the manufacturing process, or vacuum pump oil can change the local propellant wetting and thus the emission characteristics. In addition, manufacturing and assembly tolerances on the needle rim thickness, shield height above the needle tip, and hole alignment must be very small to ensure reproducibility of results. The contamination and tolerance problems lead to a nonuniformity of emitters and thus a velocity decrease and disparity which affects both the specific impulse and efficiency.

A second contamination problem, that of tar buildup on the needle tips due to bombardment by secondary electrons from the extractor, has apparently been resolved by careful control of the shield height and by dimpling the extractor between apertures. Also, by careful propellant and vacuum management, propellant "pullback" has been demonstrated.³¹

To reduce the mechanical complexity of delivering both propellant and high voltage and of aligning each of the 432 needles of this 4.4-mN (1.0-mlb) thruster, and to increase the reliability and thrust per unit exhaust area, two parallel efforts to develop large high-thrust-density colloid emitters are in progress. One of these emitters, of a tubular design, is shown in Fig. 11b, whereas a standard needle is shown in Fig. 11a. The emitter consists of a 0.1-mm-i.d. capillary tube, which opens up to a 2.28-mm-i.d. cup, the rim of which acts as the emitter.³³ The shield and extractor electrodes are not shown for the tubular emitter. The shield electrode has been sectioned into three deflector electrodes. Separately biasing these three deflectors up to several thousand volts with respect to the emitter electrostatically vectors the exhaust beam up to 17.5° from the thruster axis. Early tests with a four-source array of these emitters (shown in Fig. 12), gave performance measurements of 550 μ N (124 μ lb) thrust, 13000 m/sec effective exhaust velocity (1330 sec), and 75% efficiency as measured by a time-of-flight technique during a 100-hr test. Recent data from a three-source array on a thrust stand yielded 445 μ N (100 μ lb) thrust, 10,800 m/sec effective

**Fig. 11 Colloid emitters.****Fig. 12 Tubular colloid emitter array (TRW).**

exhaust velocity (1100 sec), and 64% beam efficiency. Comparative time-of-flight data give 440 μ N (99 μ lb) thrust, 13,200 m/sec effective exhaust velocity (1350 sec), and 76% efficiency with a mass-to-charge ratio of $1.56 (10^4)$ amu/e.³⁴

Another high-thrust density emitter of a different configuration is shown in Fig. 11c. In this configuration, an approximately 0.0076-mm-wide emitting annulus is formed by two nominally 1.27-cm-i.d. concentric tubes with an inner spherical extractor electrode centrally located inside the inner tube.³⁵ The outer extractor electrode is of conventional design and is not shown in the figure. Electrostatic thrust vectoring of up to 7.5° has also been demonstrated with this emitter, in this case by separately biasing the quadrants of the outer extractor electrode. Using time-of-flight data, a single source of this type has been shown to provide a thrust of 112 μ N (25.1 μ lb), an effective exhaust velocity of 11,400 m/sec (1160 sec), and an efficiency of 63% in a 1023-hr test using a propellant doped with lithium iodide.³⁶ A three-source closely-packed array, (Fig. 13), has been shown to provide 445 μ N (100 μ lb) thrust, 13,700 m/sec effective exhaust velocity (1400 sec) and 72% efficiency, again using the time-of-flight technique.³⁷

Ion Thrusters

The ion engine generates thrust by accelerating discrete propellant ions electrostatically. With reference to Fig. 14,

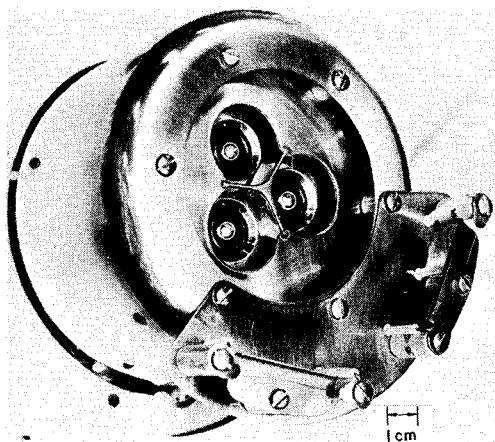


Fig. 13 Annular colloid emitter array (EOS).

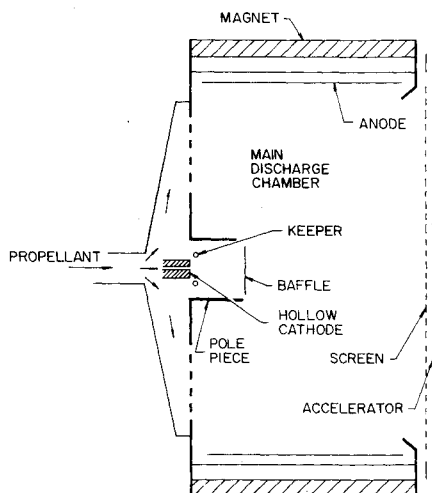


Fig. 14 Schematic of ion engine.

propellant atoms injected into the chamber through the rear wall are ionized by an electrical discharge generated between a central hollow cathode and a cylindrical anode. The efficiency of creating the ions by electron collisions is enhanced by an applied axially divergent magnetic field formed by pole pieces at the downstream end of the anode and around the hollow cathode. The downstream end of the chamber is fitted with a screen electrode maintained at approximately the same positive potential as the cathode. Ions passing through the screen are accelerated in an electric field formed by a negatively biased accelerator grid mounted less than one millimeter downstream of the screen grid. A second, smaller hollow cathode, positioned immediately downstream of the accelerator grid and to the side of the exit beam, supplies electrons to maintain space-charge and current neutrality.

Hollow cathodes, through which a small fraction of the inlet propellant is fed, have been shown to be more efficient electron emitters and to have longer life than other types of emitters in this environment. The hollow cathode plasma is initiated and stabilized by the use of a "keeper" electrode, which draws a fraction of the emitted electron current. The "baffle" increases the voltage drop in the discharge to produce higher energy electrons which have a larger ionization cross section; in addition, it reduces the direct axial flow of neutral propellant exhausting from the cathode.

Although the thrust per unit exhaust area of the ion engine is limited by space charge considerations, this device is capable of efficient acceleration over a range of effective exhaust velocities from 20,000 m/sec up to greater than 100,000 m/sec (2000-10,000 sec). The optimum exhaust velocity is determined from system tradeoff and mission analysis studies. Unfortunately, until large, light-weight space

power supplies are developed, only the lower extent of this range will be utilized. With an appropriately sized solar array, however, the ion engine is capable of performing both high impulse auxiliary propulsion missions and modest primary propulsion missions. The past and present stable of ion thrusters reflects this wide applicability span.

Ion thrusters have been explored over a range of chamber diameters from a few cm up to 150 cm. More extensive development of a select few of these devices has led to nine separate space tests of ion engines since 1962.³⁸ One of the most notable of these tests is the SERT II flight launched in 1970.

SERT II carried two NASA Lewis Research Center 15-cm mercury electron bombardment ion thrusters into a 1000-km polar orbit. The primary goal was to demonstrate six month continuous operation in space, with a secondary objective of examining the various interactions of the thrusters with the spacecraft. Both thrusters failed to reach the six-month operational goal, due to an electrical short believed caused by erosion of the accelerator grid near the neutralizer. Nevertheless, long-term operation of the thruster was established (one unit operated for 3781 hr and the other for 2011 hr), and the erosion problem has subsequently been eliminated by repositioning the neutralizer. Other accomplishments of this flight were the agreement between flight performance data and lab performance data verifying thruster specification procedures, the restart capability of the cathode assemblies, even after 4½ years in orbit, and the absence of any significant interaction between thruster and spacecraft.

Based on the success of SERT II, the ion engine program has focused onto the 8-cm and 12-cm diam thrusters for auxiliary propulsion applications and the 30-cm diam thruster for primary propulsion mission.

8-Cm Mercury Thruster (Hughes)

The 8-cm diameter ion engine evolved from a 5-cm thruster previously developed for attitude control of satellites in the 220-680 kg class. This latter thruster reached flight qualification status and was capable of producing a thrust of 2.1 mN (0.47 mlb) at an effective exhaust velocity of 29,800 m/sec (3040 sec), an electrical efficiency of 56%, and an overall efficiency (including total propellant utilization) of 43%.³⁹ Especially notable tests performed with this thruster included a 7680-hr test of an electrostatically vectored accelerator grid and a 9715-hr test of the remaining components.⁴⁰

With the trend toward larger spacecraft, however, there followed a need for thrust levels in the 2-10 mN (0.4-2 mlb) range. This led to the present 8-cm thruster program.

The 8-cm ion engine is based on a mechanical structure similar to that of the flight-qualified 5-cm design. Termed the Structurally Integrated Ion Thruster (SIT-8), the thrust chamber is cantilevered from the main support flange, which is at the center of mass near the midplane of the mercury propellant tank.⁴¹ Figure 15 is a photograph of the thruster

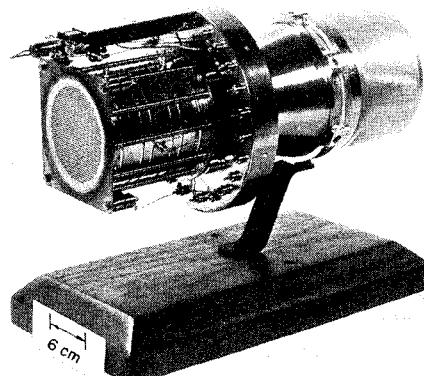


Fig. 15 SIT-8 mercury ion thruster (Hughes).

with its outer screen removed showing the thrust chamber and its cantilever mounting. The principal features which distinguish the thrust chamber from the simplified schematic shown in Fig. 14 are: 1) a dished-grid ion extraction system to maintain the close tolerances on the grid spacing under conditions where thermal stresses would cause deformities; 2) a simplified hollow cathode ignition system, which utilizes a high voltage pulse to initiate the cathode emission; 3) tantalum protection on the upstream thruster endplate and the hollow cathode baffle to reduce sputtering in the discharge chamber; and 4) a screen mesh anode to contain sputtered material within the chamber. The thrust vector will be controlled in two orthogonal directions by gimbaling the entire thruster.

Performance

The performance goals for this thruster are as shown in Table 7. Preliminary data⁶ indicate that, for a thrust of 5.1 mN (1.14 mbl) at an effective exhaust velocity of 27,400 m/sec (2800 sec), a power input of 122 w (not including power conditioning losses) is required. This corresponds to a thruster efficiency of 57%.

System status

In June 1974, work began on the Engineering Model (EM) of this thruster. Performance goals remain as stated in Table 7. In addition, performance standards require a projected lifetime of 20,000 hr, a capability to undergo 10,000 restarts under space conditions, thrust vector control by gimbaling of $\pm 10^\circ$ in two orthogonal directions, a start-up time to design performance in less than 15 min., and operational characteristics which permit stable closed-loop control. A 15,000-hr cyclic test of the thruster, power conditioner, and mass feed system is planned in the near future. The expected mass distribution of the SIT-8 thruster is given in Table 8.⁴²

8-cm Cesium Thruster (EOS)

Two complete 8-cm cesium thruster systems are on the Application Technology Satellite (ATS)-6, which was launched in May 1974. Their purpose was to demonstrate long-term north-south stationkeeping of a geosynchronous satellite. The thrusters are mounted on the north and south faces of the satellite such that their thrust vectors form a 37° angle with the earth-pointing axis. The anticipated duty cycle required each thruster to operate 5-10 hr per day, depending on the disturbance torques.⁴³

The complete thruster subsystem and the control logic and power conditioning sub-system are shown in Fig. 16. The units are separately mounted on the spacecraft and connected by a 92-cm-long cable.

The thruster chamber utilizes magnetoelectrostatic confinement of the plasma.⁴⁴ In this arrangement, the magnetic

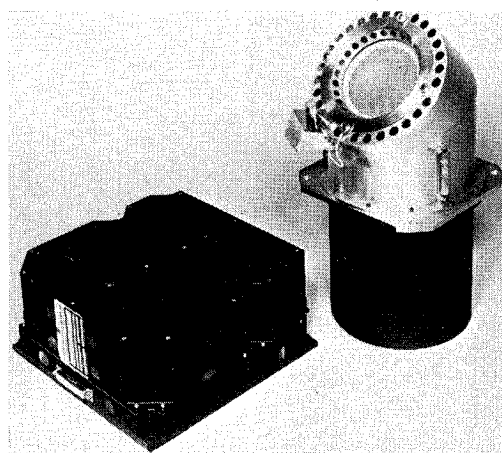


Fig. 16 8-cm cesium thruster on ATS-6 (EOS).

field is formed by magnetic strips, alternately of opposite polarity, interspersed with anode strips. This forms a magnetic barrier which limits ion and electron migration to the outer chamber wall thus decreasing ion losses, improving ionization efficiency, and generating a radially more uniform chamber plasma for efficient ion extraction.

The screen and accelerator grids are planar with thrust vector control provided by small transverse movement of the accelerator grid. A thermo mechanical mechanism provides the grid translational movement which produces $\pm 3^\circ$ thrust vector control in two orthogonal directions. A plasma-bridge neutralizer operating at spacecraft potential is located 5-cm from the accelerator electrode and points 60° downstream.

The power conditioner converts the 28-v d.c. spacecraft voltage into the requisite voltages and currents for the thruster components by using transistor inverters. Also, 13 command and 12 telemetry channels are provided. A summary of the system mass distribution is given in Table 9.⁴⁵

Performance

The 8-cm cesium thruster develops 4.45 mN (1.0 mbl) thrust with an effective exhaust velocity of 25,500 m/sec (2600 sec). The total system input power is 145 w which, with a power conditioner efficiency of 80%, delivers 123 w to the thruster. The thruster electrical efficiency is 51% and the mass utilization efficiency is 90% giving a total system efficiency of 46%. Total impulse capability is approximately 90,000 N-sec (20,200 lb-sec).

System status

Preliminary operation of the two thrusters on ATS-6 began on July 17, 1974 and October 19, 1974. Completely successful operation was achieved on the first run of each, with one thruster operating at full power for 92 hr before being shut down. In addition to verifying specified performance, the tests also demonstrated an absence of interference with the communication systems, control of spacecraft attitude by thrust vectoring, and compatibility with the star tracker. However, subsequent attempts to operate the thrusters have not been successful. Initial data analysis indicates that the problem is associated with operation of the propellant reservoirs in zero-g conditions.⁴⁶

Because the busy experiment schedule on ATS-6 precluded a two-year demonstration of north-south stationkeeping, a

Table 7 SIT-8 performance goals

Thrust, mN (mlb)	4.45 (1.0)
Effective exhaust velocity, m/sec (sec)	29,400 (3000)
Electrical efficiency, %	75
Propellant utilization efficiency, %	85
Overall efficiency, %	63
Total impulse, N-sec (lb-sec)	~ 250,000 (156,100)

Table 8 SIT-8 EM thruster mass definition

Thruster	1.4 kg
Gimbal	0.70
Propellant reservoir	1.4
Mercury propellant	8.75
Power conditioner	5.45
Miscellaneous	0.1
Total system mass	17.8 kg

Table 9 ATS-6 Cs thruster mass distribution

Thruster	2.63 kg
Propellant reservoir	1.90
Propellant	3.67
Power conditioner	7.46
Miscellaneous	0.34
Total system mass	16.00 kg

parallel life test of an identical unit was undertaken in a ground-based laboratory. In this test, the thruster operated three cycles a day, each consisting of 6 hr on and 2 hr off. The test was terminated after 471 automatic on-off cycles, during which time 2614 hr of full-thrust operation were accumulated. Cause of the termination was the failure of the neutralizer cathode heater. Postrun inspection showed negligible erosion and no other incipient failures. The cathode heaters have been modified in preparation for a two-year cyclic test.

12-Cm Cesium Thruster (EOS)

The 12-cm cesium thruster has been developed by EOS with INTELSAT funds for north-south stationkeeping of synchronous communication satellites in the 1000-kg class. Like the 8-cm cesium device on ATS-6, the thrust chamber design is based on the magnetoelectrostatic confinement principle for efficient ion production.⁴⁷ The grids are dished, with thrust vector control of up to 7° obtained by mechanical displacement of the accelerator grid with respect to the screen grid. The thruster is shown in Fig. 17.

The power conditioning unit operates with a 80-100 v d.c., 2.4-7.3-amp input from a battery which is slowly charged from the spacecraft solar array. The present unit is in the breadboard stage, with the final efficiency expected to be 90%.

Performance

The performance range accessible to this thruster includes a thrust of 10-24 mN (2.2-5.4 mlb), an effective exhaust velocity of 27,400-37,200 m/sec (2800-3800 sec), and a mass utilization of approximately 95%. Recent data include the following typical operating point: a thrust of 17.0 mN (3.82 mlb), an effective exhaust velocity corrected for total mass efficiency of 32,000 m/sec (3270 sec), an electrical efficiency of 81%, and a mass utilization (including neutralizer flow) of 97%. The associated power to the thruster is 339 w, which translates into a power-to-thrust ratio of 19.9 w/mN.⁴⁸ The total impulse capability depends on the particular mission, but is projected to be 300,000 N-sec (67,400 lb-sec) for a 5000-hr mission.⁴⁹

System status

The Engineering Model (EM) of the 12-cm-thruster has been built and performance mapped, with the next goal a 1000-hr break-in test. Total mass of the thruster system is estimated to be 21 kg, which is based on an actual EM thruster mass of 2.4 kg and estimated masses of the cesium propellant, tankage, and power conditioning of 9.5, 1.0, and 8.0 kg, respectively.

30-Cm Mercury Thruster (Hughes)

The only thruster now under development for primary propulsion in the United States is the 30-cm mercury ion engine. The performance goals for the most advanced version of this thruster, the Engineering Model (EM) thruster, are given in Table 10.⁵⁰ In addition, this thruster will have the capability of throttling down from 2.75 kw to 1.4 kw and have an operating life of more than 10,000 hr.

Table 10 30-cm EM thruster performance goals

Beam current, amp	2
Net accelerating voltage, v	1100
Thrust, N (lb)	0.135 (0.0303)
Effective exhaust velocity, m/sec (sec)	29,400 (3000)
Maximum power input, kw	2.75
Power-to-thrust ratio, w/mN	20.4
Propellant efficiency, %	91
Overall efficiency, %	73
Maximum thruster mass, kg	6.9

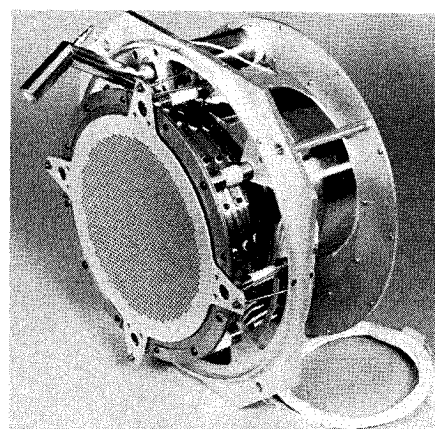


Fig. 17 12-cm cesium thruster (EOS).

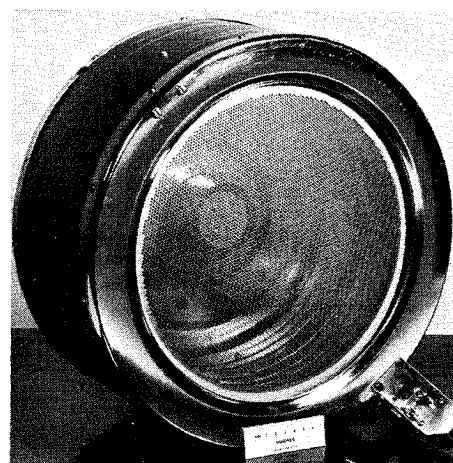


Fig. 18 30-cm mercury thruster (Hughes).

For advanced missions, ion engines of this size will be clustered and driven by large, light-weight solar arrays of up to 25 kw output. Present missions considered for the first application of this engine are a Comet Encke rendezvous, an out-of-the-ecliptic probe, and a geocentric satellite-raising mission (SERT III).

The EM thruster design does not vary markedly from the simple schematic shown in Fig. 14. The thruster has a two-point mounting consistent with thrust vector control by gimbals. The grid system consists of two molybdenum plates of 0.05- and 0.04-cm thickness, dished with the convex side out, and separated by 0.06 cm. The plates are held to a close tolerance by hydroforming with the 10,000 or more pairs of holes photochemically etched into the blanks. To compensate for the radially outward velocity component imparted by the dished grids, hole pairs are misaligned slightly so that the emerging beamlet from each pair is parallel to the thruster axis. The dished grids are more mechanically and thermally stable, provide a high current extraction capability, and reduce the discharge chamber losses to 185 ev/ion.

The hollow cathode for the discharge chamber is a 0.635-cm-diam tantalum tube with a 0.152-cm-thick thoriated tungsten end cap in which a nominally 0.076-cm-diam chamfered hole has been drilled. By increasing the diameter of the end cap beyond the tantalum tube diameter, radiative cooling maintains the tip at a temperature less than 900°C. For tip temperatures less than 1100°C, separate tests have shown that a cathode life of greater than 20,000 hr can be expected.⁶

The neutralizer hollow cathode is of comparable dimensions except for the orifice, which is approximately half the diameter. The correct heat balance is provided by allowing the cathode to radiate without heat shielding. Thus, a tip radiator, as used on the main cathode, is not required. This

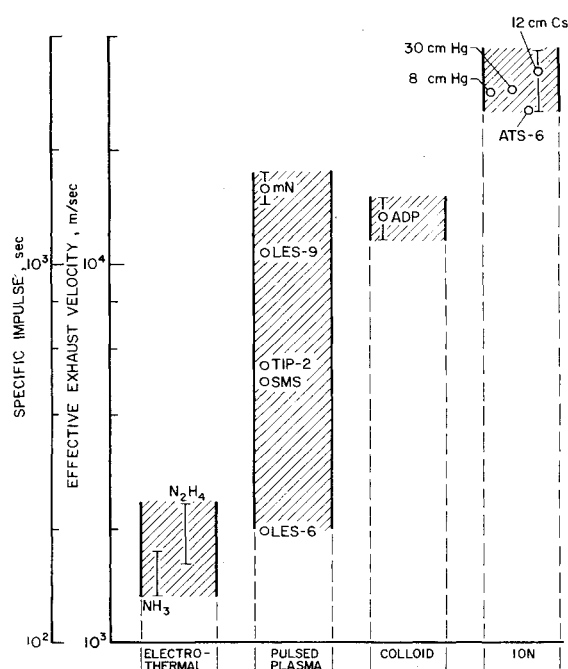


Fig. 19 Effective exhaust velocity of existing and projected systems.

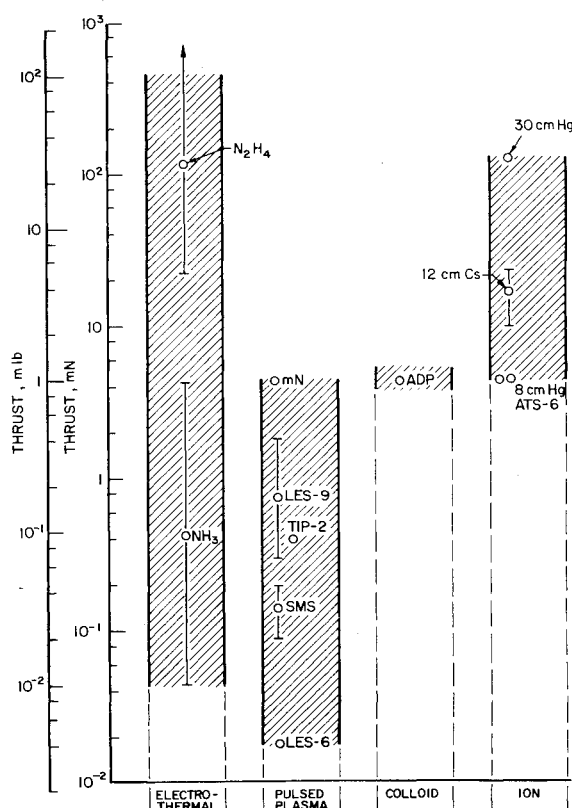


Fig. 20 Thrust of existing and projected systems.

hollow cathode is located 6.35 cm downstream of and 12.7 cm radially outward from the last row of holes in the accelerator grid, a position found from empirical tests to eliminate the grid erosion problem encountered in SERT II.⁶ The complete thruster, whose mass is 7.7 kg, is shown in Fig. 18.

The power conditioner for the 30-cm thruster processes the 200-400 v d.c. input power with inverters which use either transistors⁵¹ or thyristors⁵² for the main switching elements. The design goals for this power conditioner are an efficiency of 92% at an input power of 3 kw and a mass of 15.5 kg.⁵ The control system will allow completely automatic start-up and

continuously variable automatic thruster throttling from a single control over a range in excess of 5:1.⁵³

Performance

Preliminary performance data for the EM thruster, including throttling data, are shown in Table 11, which can be compared with the design specifications in Table 10.⁵⁰

In Table 11 the beam voltage was increased at the lower powers to keep the effective exhaust velocity approximately constant; this accounts for the increased electrical efficiencies at lower power. In addition, the propellant utilization efficiencies include the neutralizer flow and the effect of beam divergence and doubly charged ions.⁵⁴ As an example of the magnitude of these effects, the full-power propellant efficiency calculated without beam divergence and doubly-charged ions is 94.1% and the related total efficiency is 78.7%.

System status

The principal goal of the EM thruster program is the final technical verification of the 30-cm thruster before use on a mission. Perhaps the most crucial elements of the design are the grids. Through various tests of performance parameters and durability, a total of 36 different grid sets have been operated for a total accumulated time of 14,000 hr. The projected life of the grids is now more than 15,000 hr for a 2-amp beam of mercury ions accelerated to 30,000 m/sec. Additional confidence in the grids and related neutralizer placement has been gained from an 1100-hr test of the complete thruster in which negligible erosion was observed.³⁸

At present, an EM thruster is undergoing endurance testing using a fully automatic control system. As of March 6, 1975, this test had accumulated 8600 hr, which surpasses the planned goal of 7700 hr.⁵⁵

The next milestone in the qualification program of the EM thruster is a 15,000-hr test to be initiated in 1976. The goal for complete technology readiness of the 30-cm thruster system is 1979.

Technology

Although the ion thruster systems are relatively complex compared to some of the other types of electric propulsion, the technology for complete development and application of these devices seems well in hand. Desirable thruster performance has been demonstrated for both auxiliary and primary ion thrusters, and life tests show that the required durability will soon be realized. Power conditioner units have exhibited efficiencies as high as 90%, and the estimated reliability of the present 30-cm thermal vacuum breadboard model is 0.96 for 10,000-hr operation. In addition, complete closed-loop, computer control of a thrust subsystem has been demonstrated by Hughes and the Jet Propulsion Laboratory for thruster startup, transient correction, and throttling.⁴²

Further consideration of xenon as an alternate ion engine propellant may be necessary to minimize the environmental effects of mercury and cesium thrusters in geocentric missions. Tests with xenon in the 30-cm engine show a per-

Table 11 Preliminary EM thruster performance data

	Full power	¾ power	½ power
Beam current, amp	2.00	1.45	0.85
Net accelerating voltage, v	1100	1150	1350
Thrust, N	0.132	0.099	0.063
Effective exhaust velocity, m/sec	28,400	28,600	27,450
Power input, kw	2.63	1.99	1.34
Power-to-thrust ratio, w/mN	19.9	20.1	21.2
Electrical efficiency, %	83.6	83.9	85.7
Propellant efficiency, %	87.3	86.8	76.9
Overall efficiency, %	71.2	71.2	64.5

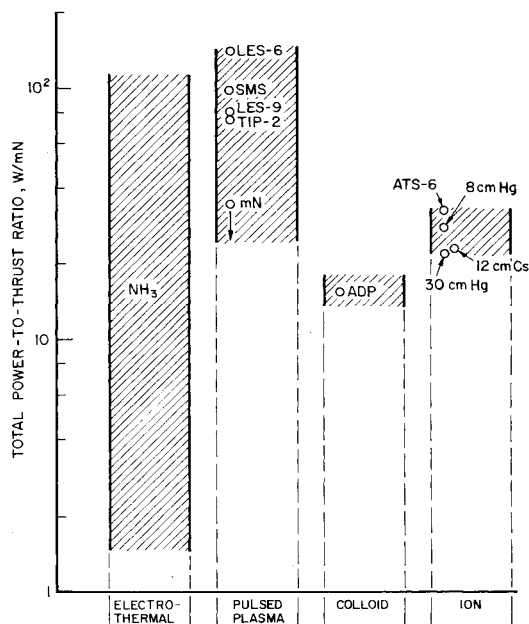


Fig. 21 Power-to-thrust ratio for existing and projected systems.

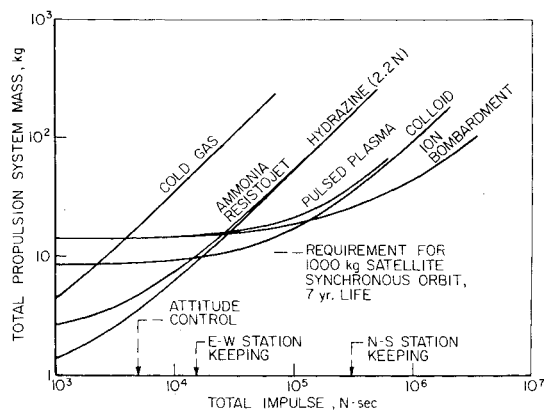


Fig. 22 Comparison of total propulsion system mass for single 4.45-mN (1-mlb) thruster systems.

formance similar to that with mercury, but with a 10-20% increase in power-to-thrust ratio due to the lower ion mass. Initial calculations indicate that, with high-pressure propellant storage, the mass of a xenon thruster system would be comparable to that of a mercury system.⁵⁶

Summary

To facilitate a comparison of the electric thruster systems discussed in this paper, the effective exhaust velocity and thrust level of the existing and projected systems are shown in Figs. 19 and 20, respectively. It is interesting to note that electric propulsion offers the spacecraft planner a range of effective exhaust velocities from under 2000 m/sec (about 200 sec) to greater than 30,000 m/sec (about 3000 sec) with an accompanying thrust variation of nearly four orders of magnitude, from less than 50 μ N (about 10 μ lb) to about 500 mN (100 mlb).

The electrical power required to produce this performance is shown in Fig. 21 for the same thruster systems. In this figure, the total system power has been used rather than just the power into the thruster, i.e., the power conditioning efficiency has been included. For most systems, this information appears in the appropriate sections of the paper; for a few, the power conditioning efficiency had to be assumed (8-cm mercury ion thruster—85%, 12-cm cesium ion thruster and 30-cm mercury ion thruster—90%). It is seen

that except for the electrothermal thrusters, the total power-to-thruster ratio of present systems covers the range from 15 to about 100 w/mN. In the case of the electrothermal thrusters, the low power-to-thrust ratios result from the relatively large proportion of cold-flow thrust for certain operating conditions.

Direct comparison of thruster system mass is difficult since each system has been optimized for a specific mission. One of the few places where a meaningful comparison can be made is among the various 4.45-mN (1-mlb) thrust systems. Figure 22 shows the total propulsion system mass including solar array mass as a function of the total impulse delivered for several electric systems as well as for a cold gas system.^{57,58} All systems have a thrust of 4.45 mN (1-mlb) except the hydrazine system whose thrust is 2.2 N (0.5 lb). The graphs were drawn by using the fixed mass components, as determined at the principal design point discussed in the paper and extrapolating the propellant mass and appropriate tankage to other total impulse situations.

For low total impulse missions such as attitude control, only the electrothermal thrusters offer a distinct advantage over cold gas systems, due to the large fixed masses of the plasma, colloid, and ion systems. For higher total impulse applications, the higher exhaust velocity systems offer a significant mass savings over all other systems. Regardless of the particular mission, Fig. 22 shows that proper selection and design of an electric thruster system can provide large benefits to the spacecraft designer.

References

- Holcomb, L. G., "Survey of Satellite Auxiliary Propulsion Systems," *Journal of Spacecraft and Rockets*, Vol. 9, March 1972, pp. 133-147.
- Kaufman, H. R. and Reader, P. D., "Electrostatic Thrusters," AIAA Paper 72-1123, New Orleans, La., 1972.
- Greco, R. V., Bliss, J. R., Murch, C. K., and Clark, K. E., "Resistojet and Plasma Propulsion System Technology," AIAA Paper 72-1124, New Orleans, La., 1972.
- Lazar, J. and Mullin, J. P., "NASA Overview of Electric Propulsion," AIAA Paper 72-1127, New Orleans, La., 1972.
- Lazar, J., "Electric Propulsion Status and Development Plans—NASA Programs," AIAA Paper 73-1143, Stateline, Nev., 1973.
- Finke, R. C. and Murch, C. K., "Current Technology in Ion and Electrothermal Propulsion," AIAA Paper 73-1253, Las Vegas, Nev., 1973.
- Rosen, S. G., "Colloid and Pulsed Plasma Thrusters for Spacecraft Propulsion," AIAA Paper 73-1254, Las Vegas, Nev., 1973.
- Greenwood, S. W., "Definition of Specific Impulse," *Journal of Spacecraft and Rockets*, Vol. 12, Jan. 1975, p. 62.
- Jahn, R. G., *Physics of Electric Propulsion*, McGraw-Hill, New York, 1968.
- Holcomb, L. B., "Satellite Auxiliary Propulsion Selection Techniques—Addendum: Survey of Auxiliary Electric Propulsion Systems," NASA/JPL Tech. Rept. 32-1505, 1971.
- Yoshida, R. Y., Halbach, C. R., and Hill, C. S., "Life Test Summary and High Vacuum Tests of 10-Mlb Resistojets," *Journal of Spacecraft and Rockets*, Vol. 8, April 1971, pp. 414-416.
- Pugmire, T. K., AVCO Corp., Systems Division, private communication, June 1974.
- Hawk, C. W., Baty, R. S., Rosen, S. G., and Quirk, J. A., "System Study of Electric Propulsion for Military Space Vehicles," AIAA Paper 72-493, Bethesda, Md., 1972.
- Murch, C. K. and Hunter, C. R., "Electrothermal Hydrazine Thruster Development," AIAA Paper 72-451, Bethesda, Md., 1972.
- Kuenzly, J. D., "Study of Monopropellants for Electrothermal Thrusters," TRW Rept. 22409-6014-RU-00, March 1974, Redondo Beach, Calif.
- Guman, W. J. and Nathanson, D. M., "Pulsed Plasma Microthruster Propulsion System for Synchronous Orbit Satellite," *Journal of Spacecraft and Rockets*, Vol. 7, April 1970, pp. 409-415.
- Guman, W. J. and Williams, T. E., "Pulsed Plasma Microthruster for Synchronous Meteorological Satellite (SMS)," *Journal of Spacecraft and Rockets*, Vol. 11, Oct. 1974, pp. 729-731.

¹⁸Vondra, R. J. and Thomassen, K. I., "A Flight-Qualified Electric Thruster for Satellite Control," *Journal of Spacecraft and Rockets*, Vol. 11, Sept. 1974, pp. 613-617.

¹⁹Guman, W.J., Fairchild Republic Co., Farmingdale, N.Y., private communication, July 1974.

²⁰Palumbo, D. J. and Guman, W. J., "Continuing Development of the Short-Pulsed Ablative Space Propulsion System," AIAA Paper 72-1154, New Orleans, La., 1972.

²¹Palumbo, D. J. and Guman, W. J., "Pulsed Plasma Propulsion Technology," AFRPL-TR-73-79, Sept. 1973, Air Force Rocket Propulsion Lab., Wright-Patterson Air Force Base, Ohio.

²²Guman, W.J., "Development of a Short Pulsed Solid-Propellant Plasma Thruster," Final Rept. MS 172R0001, March 1974, Fairchild Republic Co., Farmingdale, N.Y.

²³Clark, K. E. and Jahn, R. G., "Quasi-Steady Plasma Acceleration," *AIAA Journal*, Vol. 8, Feb. 1970, pp. 216-220.

²⁴Jahn, R. G., Clark, K. E., Oberth, R. C., and Turchi, P. J., "Acceleration Patterns in Quasi-Steady MPD Arcs," *AIAA Journal*, Vol. 9, Jan. 1971, pp. 167-172.

²⁵Saber, A. J. and Jahn, R. G., "Anode Power Deposition in Quasi-Steady MPD Arcs," AIAA Paper 73-1091, Stateline, Nev., 1973.

²⁶Burkhart, J. A., "Exploratory Tests on a Downstream Cathode MPD Thruster," *Journal of Spacecraft and Rockets*, Vol. 8, March 1971, pp. 240-244.

²⁷Burkhart, J. A., "Performance of a Modified Downstream Cathode MPD Thruster," *Journal of Spacecraft and Rockets*, Vol. 10, Jan. 1973, pp. 86-88.

²⁸Daily, C. L., Davis, H. A., and Hayworth, B. R., "Pulsed Plasma Propulsion Technology," AFRPL-TR-73-81, July, 1973, Air Force Rocket Propulsion Lab., Wright-Patterson Air Force Base, Ohio.

²⁹Daily, C. L., "Magnetic Field Annihilation of Impulsive Current Sheets," AFOSR-TR-73-0564, March 1973, Air Force Office of Scientific Research, Washington, D. C.

³⁰Zafran, S., et al., "One-Millipound Colloid Thruster System Development," *Journal of Spacecraft and Rockets*, Vol. 10, Aug. 1973, pp. 531-533.

³¹Jackson, F. A., "Progress in the Development of a One-Millipound-Thrust Colloid Propulsion System," *IEEE and UKAEA Conference on Electric Propulsion of Space Vehicles*, Culham, England, April 1973.

³²Kidd, P. W. and Shelton, H., "Life Test (4350 Hr) of an Advanced Colloid Thruster Module," AIAA Paper 73-1078, Stateline, Nev., 1973.

³³Huberman, M. N. and Rosen, S. C., "Advanced High-Thrust Colloid Sources," *Journal of Spacecraft and Rockets*, Vol. 11, July 1974, pp. 475-480.

³⁴Zafran, S., TRW, Inc., Systems Group, private communication, June 1974, Redondo Beach, Cal.

³⁵Mahoney, J. F., Daley, H. L., and Perel, J., "Performance of Colloid Annular Emitters," AIAA Paper 73-1076, Stateline, Nev., 1973.

³⁶Perel, J., Mahoney, J. F., and Daley, H. L., "Duration Test of an Annular Colloid Thruster," AIAA Paper 72-483, Bethesda, Md., 1972.

³⁷Daley, H. L., Mahoney, J. L., and Perel, J., "Colloid Annular Array Thruster Development," AIAA Paper 73-1077, Stateline, Nev., 1973.

³⁸Molitor, J. H., "Ion Propulsion Flight Experience, Life Tests, and Reliability Estimates," *Journal of Spacecraft and Rockets*, Vol. 11, Oct. 1974, pp. 677-685.

³⁹Hyman, J., Jr., "Development of a 5-Cm Flight-Qualified Mercury Ion Thruster," *Journal of Spacecraft and Rockets*, Vol. 10, Aug. 1973, pp. 503-509.

⁴⁰Nakanishi, S. and Finke, R. C., "A 9700-Hr Durability Test of a 5-Cm-Diam Ion Thruster," *Journal of Spacecraft and Rockets*, Vol. 11, Aug. 1974, pp. 560-566.

⁴¹Hyman, J., Jr. and Poeschel, R. L., "Satellite Control Mercury Ion Thruster," AIAA Paper 73-1132, Stateline, Nev., 1973.

⁴²Molitor, J. H., Hughes Research Labs., private communication, June 1974, Los Angeles, Cal.

⁴³James, E. L., et al., "A North-South Stationkeeping Ion Thruster System for ATS-F," AIAA Paper 73-1133, Stateline, Nev., 1973.

⁴⁴Ramsey, W. D., "12-Cm Magneto-electrostatic Containment Mercury Ion Thruster Development," *Journal of Spacecraft and Rockets*, Vol. 9, May 1972, pp. 318-321.

⁴⁵Worlock, R. M., Electro-Optical Systems, Systems Division, private communication, June 1974.

⁴⁶Worlock, R. M., et al., "The Cesium Bombardment Engine North-South Stationkeeping Experiment on ATS-6," AIAA Paper 75-363, New Orleans, La., 1975.

⁴⁷Ramsey, W. D. and James, E. L., "A Prototype North-South Stationkeeping Thruster," AIAA Paper 74-1119, San Diego, Calif., 1974.

⁴⁸James, E. L. and Ramsey, W. D., "A Prototype 12-Centimeter Cesium Ion Thruster for North-South Stationkeeping," AIAA Paper 75-387, New Orleans, La., 1975.

⁴⁹Free, B. A., Comsat Labs., private communication, June 1974.

⁵⁰Poeschel, R. L., King, H. J., and Schnelker, D. E., "An Engineering Model 30-Cm Ion Thruster," AIAA Paper 73-1084, 1973.

⁵¹Herron, B. G., Collett, C. R., and Garth, D. R., "Development, Integration, and Testing of a 30-Cm Thruster/Power Conditioning and Control System," AIAA Paper 72-509, Bethesda, Md., 1972.

⁵²Biess, J. J., et al., "Thyrister Power Processor for the 30-Cm Mercury Electric Propulsion Engine," AIAA Paper 75-433, New Orleans, La., 1975.

⁵³Herron, B. G., Worden, J. D., and Simpkins, J. M., "A 30-Cm Thruster Power Processor Test Console," AIAA Paper 73-1104, Stateline, Nev., 1973.

⁵⁴Vahrenkamp, R. P., "Measurement of Double-Charged Ions in the Beam of a 30-Cm Mercury Bombardment Thruster," AIAA Paper 73-1057, Stateline, Nev., 1973.

⁵⁵Collett, C. R., "A 7700-Hr Endurance Test of a 30-Cm Kaufman Thruster," AIAA Paper 75-366, New Orleans, La. 1975.

⁵⁶Owens, W. L., Jr., "A Noble Gas Ion Propulsion System," AIAA Paper 73-1114, Stateline, Nev. 1973.

⁵⁷Owens, W. L., Jr., "Optimization of Ion Propulsion for N-S Stationkeeping of Communications Satellites," AIAA Paper 72-1150, New Orleans, La., 1972.

⁵⁸Owens, W. L., Jr., Lockheed Missiles and Space Co., private communication, Sunnyvale Calif., July 1974.